Liposomal delivery of hydrophobic RAMBAs provides good bioavailability and significant enhancement of retinoic acid signalling in neuroblastoma tumour cells

Maja Bilip[1], Shreya Shah[1], Mayuran Mathiyalakan, Aristides Tagalakis[2], Stephen L. Hart, Ruhina Maeshima, Simon Eaton, Michael Orford, Elsa Irving, Alessia Di Florio, Claire Simons* and Andrew W Stoker

Great Ormond Street Institute of Child Health, UCL, 30 Guilford St., London WC1N 1EH, UK

*School of Pharmacy and Pharmaceutical Sciences, College of Biomedical and Life Sciences, Cardiff University, King Edward VII Avenue, Cardiff CF10 3NB, UK

[1] equal first author

Corresponding author: Andrew W Stoker

Orchid ID : https://orcid.org/0000-0001-8902-5682

Address: Great Ormond Street Institute of Child Health, UCL, 30 Guilford St., London WC1N 1EH, UK; Email: a.stoker@ucl.ac.uk; tel: 0044(0)207905 2244

Current address: [2] Edge Hill University, Department of Biology, Ormskirk, L39 4QP, UK

Liposomal delivery of hydrophobic RAMBAs provides good bioavailability and significant enhancement of retinoic acid signalling in neuroblastoma tumour cells

Abstract

Retinoid treatment is employed during residual disease treatment in neuroblastoma, where the aim is to induce neural differentiation or death in tumour cells. However, although therapeutically effective, retinoids have only modest benefits and suffer from poor pharmacokinetic properties. *In vivo*, retinoids induce CYP26 enzyme production in the liver, enhancing their own rapid metabolic clearance, while retinoid resistance in tumour cells themselves is considered to be due in part to increased CYP26 production. Retinoic acid metabolism blocking agents (RAMBAs), which inhibit CYP26 enzymes, can improve retinoic acid pharmacokinetics in pre-clinical neuroblastoma models. Here we demonstrate that in cultured neuroblastoma tumour cells, RAMBAs enhance retinoic acid action as seen by morphological differentiation, AKT signalling and suppression of MYCN protein. Although active as retinoid enhancers, these RAMBAs are highly hydrophobic and their effective delivery in humans will be very challenging. Here we demonstrate that such RAMBAs can be loaded efficiently into cationic liposomal particles, where the RAMBAs achieve good bioavailability and activity in cultured tumour cells. This demonstrates the efficacy of RAMBAs in enhancing retinoid signaling in neuroblastoma cells and shows for the first time that liposomal delivery of hydrophobic RAMBAs is a viable approach, providing novel opportunities for their delivery and application in humans.

Keywords: neuroblastoma, retinoic acid, liposome, RAMBA, CYP26, neural differentiation

Abbreviations: RAMBA, retinoic acid metabolism blocking agent; ATRA, all-trans retinoic acid; 13-cis-RA, 13-cis retinoic acid

Introduction

Neuroblastoma is a paediatric, peripheral nervous system cancer, accounting for 15% of childhood cancer deaths [1] and it presents a stubborn clinical challenge. In aggressive disease, multimodal treatments are followed by maintenance treatment for residual disease, which includes the vitamin A derivative, retinoic acid (RA) [2]. RA induces neuroblastoma tumour cell differentiation or death in a range of neuroblastoma-derived cells in culture [3,4]. Although it is uncertain exactly how RA influences tumour cell behaviour in patients, the treatment does provide modest improvements in event-free survival [2,5]. Nevertheless, the approach of dosing infants and young children with 13-cis retinoic acid (13-cis-RA) is challenging, with sub-optimal exposure [2,6] and dose-limiting toxicities [2,6]. RA action *in vivo* is further hampered by its rapid metabolism by cytochrome P450 enzymes in the liver and the tumour [7]. Chronic induction of P450 enzymes may also underlie a proportion of RA resistance cases [8,9]. Further improvements in RA efficacy *in vivo* are therefore needed and this could be relevant to a range of cancers where retinoids are employed therapeutically [10,11].

In neuroblastoma treatment, 13-cis-RA is viewed as a pro-drug, with its isomer, all-trans RA (ATRA), being the biological effector inside cells [12,13] [14]. ATRA transcriptionally auto-induces P450 enzymes of the CYP26 subclass, triggering its own destruction. These enzymes have thus become druggable targets of interest, since they are largely responsible for RA clearance during treatment (Thatcher and Isoherranen, 2009). CYP26 inhibitors are known as RA metabolism blocking agents (RAMBAs) and they hold the potential of improving the clinical benefit of retinoid treatments. Numerous RAMBAs exist [15,16,17 ,18-20] and these can raise the effective intracellular concentrations or serum concentrations of RA [18,21]. One of these, liazorole, decreases the induced loss of ATRA in serum in acute promyelocytic leukemia patients [22], suggesting a potential approach for

suppressing retinoid resistance. Another RAMBA, R116010, is highly CYP26-specific with low IC_{50} and good anti-tumour activity in RA-treated breast cancer models [13,23,24]. R116010 also blocks CYP26 action both in SH-SY5Y neuroblastoma cells and in the liver, leading to increased serum levels of both ATRA and 13-cis-RA in mice [18]. It is possible therefore that RAMBAs could enhance retinoid action in neuroblastoma tumour cells themselves, inducing differentiation, cell death and N-Myc suppression, although this has not been demonstrated directly.

To further improve the pharmacokinetics of retinoids *in vivo*, there is a need for more effective delivery systems for some of the most potent RAMBAs. In this study we have used RAMBAs based on imidazole (RAMBA C2) and on triazole (RAMBA C17), these having similar, high specificities and *in vitro* EC_{50} values to R116010 [19,20]. C2 and C17, however, are highly hydrophobic compounds and impractical for use in standard oral or intravenous delivery and are therefore not suitable as drugs in this form. Improved delivery and targeting of drugs can nevertheless be achieved using nanotechnology, as evidenced in pre-clinical data using several drugs in neuroblastoma [25-27] and other solid tumours [28]. Liposomes for example have successfully enhanced drug actions by improving stability, serum longevity and therapeutic efficacy [29]. They are suitable for hydrophobic compounds and may also override drug resistance mechanisms [30,31]. Nanoparticles are also known to take advantage of tumour vascular leakiness to more specifically access tumour cells in solid tumours including neuroblastoma [25,28,32]. For RAMBAs this approach has not been documented to date and we hypothesised that liposomal delivery would improve bioavailability and making such compounds more accessible for use in humans. Our experimental model in cultured tumour cells would thus provide a proof of principle that could potentially augment future application of RAMBA-based therapy in vivo.

The objectives in this study were therefore to first demonstrate the effectiveness of RAMBAs in enhancing a range of RA actions in neuroblastoma cells, and then to provide a

proof of principle that RAMBAs can be effectively delivered to tumour cells using liposomal systems.

Materials and Methods

Chemicals and antibodies

Chemicals were from Sigma Aldrich unless otherwise stated. ATRA and 13-cis-RA (Sigma-Aldrich) were dissolved in either ethanol or DMSO at 10mM or 50mM, respectively, and protected from light at -20^{o}C. RAMBAs methyl 2,2-dimethyl-3-[4-(naphthalen-2-ylamino)phenyl]-3-(1*H*- 1,2,4-triazol-1-yl)propanoate [compound 17; C17; molecular weight 400.5] and methyl 3-(1*H*-imidazol-1-yl)- 2,2-dimethyl-3-(4-(naphthalen-2-ylamino)phenyl)propanoate [compound 2; C2; molecular weight 399.5] were generated as described [19] and were dissolved in ethanol at 50mM (C17) and 1mM (C2; maximal solubility in this solvent). Antibodies were sourced as follows: anti-N-myc (B8.4.B; Insight Biotechnology); anti-phospo-Ser472-AKT (ab4060; Cell Signaling Technology); anti-AKT (ab9272; Cell Signaling Technology); anti-pan-TRK (sc7268 and F0908; Insight Biotechnology); anti-actin (A5316; Sigma Aldrich); anti-GAPDH (14C10; Cell Signaling Technology). HRP-linked secondary antibodies were purchased from DAKO Ltd.

Cell Culture

Human immortalised cell lines SK-N-SH and IMR32 were obtained from ATCC, KELLY/N206 were a gift from Frank Speleman, University of Ghent (STR genotyped), and LAN-5 were from the Children's Oncology Group Repository, Texas, USA. All cells have been validated by short tandem repeat profiling (LGC Standards) and are mycoplasma tested. Cells were maintained at 37°C, 5% CO_2. SK-N-SH were cultured in Minimum Essential Medium Eagle, 1% penicillin/streptomycin, 10% fetal bovine serum and 2mM L-glutamine.

LAN-5 and N206 cells were cultured in RPMI 1640+GlutaMAX™ (Invitrogen), 10% fetal bovine serum and 1% penicillin/streptomycin, with 25mM HEPES pH7 (Fisher Scientific).

Immunoblotting

Cells were lysed in 50mM Tris-Base pH7.6, 150mM NaCl, 1% Triton X-100, 1x Protease Inhibitors, 25mM sodium fluoride, 1mM sodium vanadate. Proteins were separated by polyacrylamide electrophoresis and transferred to PVDF (Immobilon-P). Immunodetection was performed using HRP-linked secondary antibodies, and Pierce ECL 2 Substrate (Thermo Scientific) and chemiluminescence film (Amersham Hyperfilm ECL, GE Healthcare).

Liposomes

The lipids 1,2-di-O-octadecenyl-3-trimethylammonium propane (DOTMA), 1,2-Dioleoyl-*sn*-glycero-3-phosphocholine (DOPC) and cholesterol were purchased from Avanti Polar Lipids. For empty liposomes DOTMA, DOPC and cholesterol were dissolved in chloroform in a final volume of 500µL at a molar ratio of 37.5% : 37.5% : 25%. RAMBA C2 and C17 were dissolved in ethanol and added at a 10% molar ratio to lipids DOTMA (35%), DOPC (35%), and cholesterol (20%). Chloroform was rotary evaporated (BÜCHI Labortechnik AG) and lipids were rehydrated in nuclease-free water, rotating overnight, to form liposomes at either 1mg/ml or 2mg/ml lipids. For the 2mg/ml mixture, this equates to the equivalent of 1.1mM DOTMA, 0.11mM DOPC and 0.64mM cholesterol, and in these liposomes the RAMBAs were packaged at a maximal potential concentration of 95.7µg per mL (0.24mM) in the liposome solution. After synthesis, liposomes were sonicated for 30-45 min, with the aim of achieving a mean size of between 80-160 nm. Size and charge were assessed with a Zetasizer Nano ZS (Malvern Panalytical, UK). Liposomes were stored at 4°C. To dialyze liposomes, slide-A-Lyzer™ MINI devices (Thermo Fisher Scientific, Massachusetts, USA; molecular

weight 10 kDa; capacity 15mL) were used with 500 µL liposomes and this was dialyzed against 13.5ml distilled water for 24 h at 4^{o}C, with one water change.

Cell viability assays

Cells were plated at 3000 cells per well in 96-well plates. After 24 hr, triplicate wells of cells were treated with chemicals and incubated for five or six days, then assayed for cell number using resazurin (R&D systems) as per the manufacturer's guidelines. Reaction product was measured using fluorescence at 540 nm excitation and 590 nm emission wavelengths, in a FLUOstar Optima (BMG Labtech, Aylesbury, UK).

Neurite outgrowth assays

Cells were treated and either then photographed live or after 4% paraformaldehyde fixation. Five to ten fields of view were captured under phase contrast per tissue culture well. Neurites greater than one cell body length were measured using the NeuroJ plugin for ImageJ and cell bodies were counted using the "point-count" function. Light microscopy was performed at the Light Microscopy Core Facility, UCL GOS Institute of Child Health. Where statistical analysis was used, a univariate ANOVA analysis was performed using SPSS with 95% confidence intervals. Post-hoc tests included a Bonferroni adjustment and a Dunnett test where stated.

Real Time PCR

LAN5 and SK-N-SH cells were plated at 3 x 10^5 per well in 6-well plates. The next day, cells were treated with 0.1µM or 0.5µM ATRA. After 72 h, RNA was extracted and DNAse treated using the TURBO DNA-*free* kit (Ambion) according to the manufacturer's recommendations. cDNA was synthesized from 1µg of total RNA using Transcriptor First Strand cDNA

synthesis (Roche) according to the manufacturer's recommendations. Real-time PCR was performed using iTaq Universal SYBR Green Supermix (Bio-Rad) in triplicate for the CYP26A1 primers (forward: GGC CTT AGG AGC TGT GTA GG; reverse: TTG TCC ACA GGA TAC ACG GT) and a GAPDH control was used for normalization (forward: ATGACATCAAGAAGGTGGC; reverse: CATACCAGGAAATGAGCTTG). The thermocycling program was one cycle at 95°C for 5 min, 95°C for 15 seconds, 60°C for 1 min, followed by 40 cycles of 95°C for 15 seconds and 60°C for 1 min (CFX96 Real- Time System, C1000 Touch Thermal Cycler, Bio-Rad). Melt curve analyses were performed from 65°C to 95°C, over 5 min. Fold changes in CYP26A1 mRNA were calculated according to the equation: $2^{(-\Delta\Delta Ct)}$.

RNAseq analysis

RNA was extracted and 250ng was processed using Illumina's TruSeq RNA sample prep kit version 2 (p/n RS-122-2001) according to the manufacturer's instructions. mRNA was isolated using Oligo dT beads and the purified mRNA was chemically fragmented. cDNA was generated using Reverse Transcriptase and random primers. Indexing Adaptors were ligated and the cDNA libraries were amplified by PCR. Samples were sequenced on a NextSeq 500 (Illumina, San Diego, US) using a 43bp paired end run. Data was converted to fastq using Illumina bcl2fastq v2 and aligned to reference using TopHat2 (http://www.genomebiology.com/2013/14/4/R36/abstract). Duplicate reads were removed (Picard v1.100) and transcript abundance estimated with Python package HTSeq (http://dx.doi.org/10.1093/bioinformatics/btu638). Differential expression was determined using DESeq2 (http://doi.org/10.1186/s13059-014-0550-8).

UV detection of RAMBA

For standard curve measurement, RAMBAs were dissolved in ethanol and scanned for absorbance from 200-450nm in a UVIKON UV spectrophotometer with Lab Power Junior software. To quantify C2 RAMBA in liposomes, the pre- and post-dialysis mixtures were diluted 1:9 with ethanol and scanned at OD_{315}. Background absorbance of the lipids was measured at OD_{315}, using empty liposomes similarly dissolved in ethanol.

Results

RAMBA induction of CPY26A1 transcription

It is unclear what pattern of expression there is of CYP26 paralogues in neuroblastoma tumour cells. We thus analyzed expression of CYP26A-C using RNAseq datasets from tumour cell lines LAN5, SK-N-SH, KELLY and IMR32 (Figure 1A). LAN5 and SK-N-SH cell samples were either untreated or treated with ATRA (5μM) for 24 h. KELLY and IMR32 samples were from untreated cells only. *CYP26C* mRNA is not detected except for very low levels in IMR32. *CYP26B1* is expressed in all lines in basal conditions and is the most abundant paralogue in KELLY and IMR32. *CYP26A1* is expressed basally in each cell type except KELLY. *CYP26B1* and *CYP26A1* are strongly induced up to 10000-fold by ATRA in LAN5 and SK-N-SH. *CYP26C1* is induced by ATRA, but only up to ten-fold, in LAN5 and SK-N-SH cells. In this study therefore, the RAMBA effects are likely to be predominantly acting through *CYP26A1* and *CYP26B1*.

In our experiments we used two RAMBA compounds, one based on an imidazole structure (C2) and one on triazole (C17) [19] (Figure 1B). C2 and C17 have IC_{50} values of 3nM and 0.35nM, respectively, against CYP26 enzymes *in vitro* and can enhance *CYP26A1* mRNA induction by ATRA in SH-SY5Y [19]. To assess RAMBA activity SK-N-SH cells (Figure 1C), cells were treated with ATRA at either 0.5μm or 0.1μM, with or without the

addition of C2 at 2μM or C17 at 1μM. When using ethanol-solubilised RAMBAs in SKNSH cells the control cells contained the equivalent amount of ethanol solvent (less than 0.2% v/v). ATRA stimulated *CYP26A1* transcription up to 1000-fold, whereas the addition of either C2 or C17 induced a 20-30-fold further stimulation of transcription. These data are therefore consistent with previous findings in SH-SY5Y [19], with the RAMBAs strongly enhancing RA's ability to stimulate *CYP26A1* transcription.

Stimulation of Morphological Differentiation by RAMBAs

RAMBAs can enhance retinoid-induced differentiation in breast cancer cells [24,33], but the equivalent biological or biochemical responses downstream of RA in neuroblastoma cells have yet to be demonstrated. A key characteristic of retinoid action in neuroblastoma cells is the induction of neuronal differentiation, characterised by highly elongated neurites with growth cones and neuron-like cell bodies [3]. To assess differentiation, C2 and C17 were used alone or in combination with ATRA to treat SK-N-SH cells. Morphological differentiation was gauged by neurite outgrowth and the neuronal cell morphology. In contrast to RAMBA on breast cancer cells [24,33], RAMBAs C2 and C17 alone had no obvious morphological effect in SK-N-SH (Figure 2A). The combination treatments of RAMBAs plus ATRA, however, consistently led to a more extreme morphological differentiation compared with ATRA alone, generating more rounded and phase-bright neurons with extensive processes compared with the more phase dark, polygonal phenotype of ATRA-treated cells (Figure 2A). These observations indicate that C2 and C17 can enhance retinoid-stimulation of morphological differentiation. Neurite length quantitation showed that RAMBAs themselves did not affect neurite outgrowth, whereas ATRA treatment did enhance outgrowth (Figure 2B). Combination treatments showed that RAMBAs enhanced this ATRA-induced neurite elongation. Increasing the concentration of C17 from 1μM to 10μM did not

further increase the neurite effect. C2 and C17 RAMBAs can thus enhance the cellular differentiation driven by ATRA in SK-N-SH cells.

Biochemical enhancement of retinoid action by RAMBAs

Retinoid stimulation of neuroblastoma cells induces a wide range of biochemical changes, including enhancement of AKT phosphorylation, which is required for neurite elongation in ATRA-treated SK-N-SH cells [34,35]. If RAMBAs can enhance the biochemical actions of ATRA, then we should observe a combination effect on AKT phosphorylation. SK-N-SH cells were treated with 0.1μM ATRA for 72 h in the absence or presence of either 0.5μM or 2μM C2. Figure 2C and 2D show that C2 can indeed enhance the level of pAKT generated by ATRA. This effect was more pronounced with the lower C2 concentration.

Delivery of RAMBAs using liposomes

So far, we have provided the first demonstration that RAMBAs C2 and C17 can enhance both the biochemical and morphological measures of ATRA signalling in SK-N-SH neuroblastoma cells. C2 and C17 can be delivered to cells after ethanol solubilisation, but their high hydrophobicity would significantly limit their use in humans. A key objective of this work was therefore to assess whether similar RAMBA bioavailability can be facilitated by incorporating these molecules into liposomal nanocomplexes. This would be a proof of principle that nanotechnology could facilitate cellular delivery of such RAMBAs, potentially increasing their therapeutic applicability.

To test liposomal delivery, the C2 and C17 RAMBAs were incorporated into liposomes composed of DOTMA, DOPC and cholesterol (molar ratios 37.5%: 37.5%: 25%) suspended in water (see Methods). These kinds of liposome formulations are very effective for cellular delivery [36][37]. After sonication, positively charged liposomes with an average

size of 91nm (C17), 123 nm (C2) and 133 nm (empty) were obtained, with average PDI values from 0.42-0.47. (Table 1). We tested only cationic liposomal formulations in order to minimise charge-dependent, non-specific uptake into cultured cells [38]. These liposome solutions would contain, maximally, 240μM of the RAMBAs and the data below are presented on the basis of this maximal, theoretical incorporation of RAMBAs into the liposomes. The tolerance of neuroblastoma cells for our liposomes allowed us to deliver up to 2μM of RAMBA without excessive liposomal cytotoxicity. At this dose of RAMBA, a final concentration of 8.3μg/ml of total lipid would be added to the media. Liposomes were left on cells for the whole treatment period, unless otherwise stated.

The C17 RAMBA liposomes were initially used to treat SK-N-SH cells, to determine cellular tolerance and enhancement of ATRA-induced differentiation. The data show that liposomal C17 enhances ATRA-induced neurite elongation as effectively as ethanol-dissolved C17 (Figure 3A; compare to Figure 2). SK-N-SH cells were also tested with RAMBA C2 packaged in liposomes (Figure 3B). As additional controls, empty liposomes were used, in media with or without added ATRA. Once again, liposome packaging of C2 permits the RAMBA to enhance the ATRA-induced neurite elongation by approximately 60% (p-value 0.06). Preliminary data from LAN5 cells, another line that differentiates in response to ATRA, show a similar trend (not shown). Liposome-treated cells again showed that RAMBA co-treatment with ATRA enhanced the morphological shift towards highly rounded cell bodies (Figure 4; compare to Figure 2). These data collectively indicate that RAMBAs C2 and C17 can be successfully delivered to neuroblastoma cells in liposomes, where they enhance ATRA-dependent differentiation to a similar level as seen with ethanol-delivered RAMBAs (compare Figure 2 with Figure 4).

Empty liposome treatment generated no morphological effects (Figure 4). However, when combined with ATRA, we did sometimes observe an increased refractility of cells, but not as extreme as with the RAMBA liposome (Figure 4). Although not currently understood,

empty liposomes may have some limited propensity to enhance ATRA, possibly by binding to retinoic acid through their positive charge or by attracting retinoic acid through its hydrophobic quality.

Liposomal RAMBAs enhance ATRA-induced AKT signalling

As shown above in Figure 2, RAMBAs can enhance pAKT levels in the presence of ATRA. To assess whether liposomal RAMBAs retain this activity, SK-N-SH cells were treated with C17 liposomes and ATRA (Figure 5A). The combination treatments again enhance pAKT levels above those seen with single treatments. Further experiments were carried out with C2 liposomes, empty liposomes and lower levels of ATRA (0.05μM) (Figure 5B). Again, the C2 liposomes specifically increased pAKT stimulation in combination with ATRA. This effect may be close to maximal with 0.5μM C2, since 2μM C2 showed a lesser stimulation of pAKT (although not statistically different from the 0.5μM mean), possibly due to mild detrimental effects of the higher lipid treatment. pAKT activation was comparable between ethanol-delivered C2 and liposomal C2 (compare Figure 5 and Figure 2C). Preliminary data using C17 also shows pAKT stimulation (Supplementary Figure 2).

N-myc suppression by RAMBAs and retinoids

C2 and C17 are capable of enhancing ATRA actions as judged by pAKT and differentiation. A further outcome of retinoid treatment in neuroblastoma cells is the suppression of N-myc protein levels [39,40]. We therefore tested whether liposomal RAMBAs were capable of enhancing N-myc suppression by ATRA. The MYCN-amplified cell line LAN5 was treated with liposomes and low levels of ATRA for 24 h. Figure 5C shows the modest N-Myc response with ATRA at this 0.05μM dose, but an enhanced suppression of N-Myc in cells treated with the ATRA and C2 liposome combination.

The collective data therefore indicate that RAMBAs encapsulated in liposomes have good bioavailability in neuroblastoma cells and are effective at augmenting ATRA signalling as evidenced by enhanced neurite elongation, AKT phosphorylation and N-myc suppression.

Sustained morphological differentiation after RAMBA liposome delivery.

Previous data in the field indicates that liposomes bind to cells maximally within 4-6 h [41,42]. We wished to test if liposomal RAMBAs retained extended activity after a short cellular treatment. We treated LAN5 cells with liposomes for 24h and this cell media was then removed and replaced with fresh media containing only ATRA. Figure 6 shows that C2 liposome pre-treatment still led to enhanced ATRA-dependent neurite elongation, 6 days after liposome removal. Thus, RAMBAs in liposomes can be delivered to these tumour cells and will trigger a sustained, combination response with ATRA for several days.

ATRA suppression of cell growth is enhanced by liposomal RAMBAs

RAMBAs enhance retinoid-induced growth suppression in breast cancer cells [24,33], but the equivalent has yet to be demonstrated in neuroblastoma cells. RA increases differentiation in some neuroblastoma cell lines and in others it can reduce proliferation as well as, or instead of differentiation. We therefore tested the ability of liposomal RAMBAs to enhance the ability of ATRA to suppression cell proliferation.

When used alone, ATRA suppressed LAN5 and KELLY cell proliferation. We also compare 13-cis-RA to ATRA, since 13-cis-RA is used clinically in neuroblastoma treatment. A broadly comparable pattern of growth suppression was observed (Figure 7A, 7B). In KELLY the EC_{50} value for ATRA was approximately 0.6µM, and 0.3µM for 13-cis-RA. In LAN5, both EC_{50} values were approximately 0.3µM. This indicates that under these conditions the two retinoids act similarly in LAN5, and in KELLY the 13-cis-RA is slightly

more effective. The 13-cis-RA is thus likely isomerised efficiently into intracellular ATRA in these cells.

The cells' responses to treatment with either empty liposomes or C2-containing liposomes were assessed. Cells were treated with 80nM or 160nM ATRA, well below its EC_{50}, for 6 days, alongside either 0.5µM C2 liposomes or the equivalent amount of empty liposomes to match the lipid dose. C2 liposomes were able to significantly suppress growth in ATRA-treated KELLY and LAN5 cells compared with minimal growth suppression by ATRA alone (Figure 7C, 7D). In ATRA-treated KELLY cells, C2 liposomal treatment suppressed growth more than the empty liposomes. In LAN5 cells, both liposome formulations somewhat suppressed cell proliferation at 0µM ATRA, although this did not reach significance. C2 liposomes plus ATRA showed a suppression of LAN5 growth compared with ATRA alone, whereas the empty liposomes did not. At higher levels of ATRA up to 1µM, the C2 liposomes could still suppress cell growth (Supplementary Figure 3). These data demonstrate that C2 liposomes can enhance the growth suppression driven by ATRA, corroborating what was found with neurite elongation, N-myc suppression and AKT activation.

C2 packaging efficiency in liposomes

The experiments described so far assumed the maximal dose estimates of C2 and C17 when encapsulated in liposomes. Maximal encapsulation, however, is not routinely achieved with lipsomal formulations. During the completion of our biochemical and cellular analyses, we were able to successfully develop a UV assay and this was used to assess the actual RAMBA concentrations in liposomal formulations.

RAMBAs were first solubilised in ethanol and UV absorbance scans were performed from 200-450nm (Figure 8A). A peak at 315nm was chosen for generating a standard curve since this wavelength showed low background absorbance by empty liposomes (see below).

To calculate the amount of C2 and C17 present in liposomes, each batch of RAMBA liposomes was dissolved in ethanol at 10% v/v, and UV scans performed (Figure 8B). Empty liposomes were similarly scanned for background subtraction. The physical parameters of these particular liposomes are given in Supplementary Table 1. Compared to the maximal theoretical packaging value of 240μM, the actual encapsulation efficiency of the RAMBAs was 64-79% for C2 and 71-91% for C17 (Figure 8B). Based on this, the doses used in our cellular experiments with liposomal RAMBAs could be overestimated from between 10% to 30%.

We also assessed RAMBA retention in the liposomes, by dialysing the liposomes over 24 h and quantifying the remaining RAMBA (Figure 8B). This showed that 72-84% of C2 remained encapsulated after dialysis, and 81-95% of C17 was retained. The C17 sample 3 was left for 4 days before dialysis and these still retained 95% of the original RAMBA, indicating that nearly all of the RAMBA is retained over this extended time period.

To test if the RAMBA liposomes retained activity after dialysis, we tested the ability of dialysed C2 liposomes to induce morphological differentiation and AKT activation. The dialysed liposomes retained their qualitative effects on ATRA-induced differentiation, generating highly rounded, phase bright neurons (Supplementary Figure 1). Biochemically, the dialysed liposomes also enhanced ATRA stimulation of pAKT levels similarly to their non-dialysed liposome counterparts over this shorter 24 hr assay (Figure 8C).

Discussion

RA has proven to be a beneficial biological therapeutic in leukaemia and neuroblastoma and in several keratinization disorders [11,43]. Although the potential clinical benefits of retinoids are broad, there are significant, practical challenges with their systemic delivery. For paediatric diseases such as neuroblastoma in particular, dosing is physically difficult and off-target toxicity is well documented [44,45]. ATRA and 13-CisRA also have poor pharmacokinetics and are metabolised *in vivo* by induced CYP26 enzymes [2,6]. Lastly, retinoid resistance often develops in cancer patients, being caused in part by sustained upregulation of the same CYP26 enzymes [7-9,46]. Given the relatively modest clinical benefit of current RA treatment in neuroblastoma [2] , there is a continued need to understand whether there is greater efficacy still be gained and where the long term potential lies.

Interest in RAMBAs in recent years has focussed on whether these RA metabolism blockers could be practicable tools for enhancing RA efficacy and reducing resistance. RAMBAs may also increase the intracellular activity of RA without significantly increasing its systemic toxicity. Previous work by Armstrong and co-workers had shown that the CYP26 inhibitor R116010, co-applied with 13-cis-RA in animals, reduces 13-Cis-RA metabolism in the liver, leading to higher levels of serum 13-cis-RA and ATRA, plus greater *CYP26A1* transcription in xenografted SH-SY5Y tumours [18]. This study demonstrated that CYP26-specific RAMBAs sustained increased 13-cis-RA levels in the blood, showing a systemic benefit. Extrapolation to humans is uncertain, however, since the specificity of R116010 towards murine CYP enzymes was questioned. Although R116010 has also been shown to suppress breast cancer cell growth [47] this drug was not developed further and clinical trials did not progress. Instead of R116010, we used RAMABA C2 and C17 here to assess RAMBA potential in cultured neuroblastoma cells. C2 has a similar IC_{50} to R116010 (3 nM), whereas the IC_{50} of C17 is ten-fold lower (0.35nM) [19]. These RAMBAs could therefore be

very effective CYP26 inhibitors for use *in vivo*, but only if they can be delivered at effective doses. However, their high hydrophobicity presents a barrier to this, and we have addressed this in this study by testing their delivery to cells using liposome nanotechnology.

RAMBAs C2 and C17 delivered after ethanol solubilization alongside ATRA, induced high levels of CYP26A1 mRNA transcription in SK-N-SH cells, agreeing with previous studies [19]. We then demonstrated for the first time that C2 and C17, when dissolved in ethanol and combined with ATRA, could stimulate ATRA-dependent neuronal differentiation as judged by increased neurite elongation, and increased pAKT activation. These RAMBAs can therefore enhance ATRA action at a morphological and biochemical level in these tumour cells. To our knowledge RAMBAs have not be delivered using nanotechnology before and we have therefore provided the first demonstration that these hydrophobic molecules can be incorporated effectively into liposomes. In such a context, they retain bioavailability and an activity that is at least comparable to that seen with their ethanol-dissolved counterparts. These liposomal RAMBAs enhanced ATRA-driven neurite extension and AKT activation in SK-N-SH cells, led to greater suppression of N-myc protein and enhanced the growth-suppressive properties of ATRA. Collectively, these data demonstrate that CYP26-specific hydrophobic RAMBAs can be effectively incorporated into liposomes where their bioavailability remains effective at enhancing ATRA actions in neuroblastoma-derived cell lines

These effects of liposomal RAMBAs were achieved using combined retinoid concentrations as low as 50-80nM in KELLY and IMR32 cells, a level that is readily achievable clinically [48] [49]. The serum levels of 13-Cis-RA given to children in current dosing regimens peaks at a mean of 2.8 µM [48] or 6.9 µM [49], depending on the study, but then drops rapidly to sub-micromolar levels within 6 hours. This raises the possibility that co-treatment with liposomal RAMBAs such as C2 or C17 may be able to prolong the effective, active dose of retinoids in cells, or may even allow lower, less toxic retinoid doses to be used

in vivo. Of perhaps more relevance, the liposomal approach, if targeted correctly, could increase the local action of retinoids while minimising off-target toxicities in normal tissues. Furthermore, our sequential treatment of cells with liposomes then with ATRA, indicated that a single liposomal delivery can generate a sustained enhancement of ATRA-induced differentiation over several days. This could be of clinical relevance if translated to a similar effect *in vivo*, as an infrequent dose of RAMBA nanocomplexes may enhance and prolong the action of the currently used, daily retinoid treatment. This warrants pre-clinical studies *in vivo* in order to test this hypothesis.

One question with RAMBAs is what their best target *in vivo* would be. For example, should they be targeted to the liver, where there is significant CYP26 induction, or to the tumours tissues? Our study was done in tissue culture, focussing on the tumour-derived cells themselves, where the RAMBAs are certainly effective. Their effectiveness systemically *in vivo* is more difficult to predict at this stage. Retinoids are efficiently destroyed in the liver and so it could be argued that RAMBAs should be targeted there in order to maintain systemic retinoid levels. Nevertheless, it may be equally effective to target the solid tumours themselves directly. The possibility of delivering RAMBAs alongside RA in combined liposome formulations should also be considered.

Although the liposomes employed in our study are conventional in design and suitable for in vitro experiments, further modifications will be required for optimal targeting in vivo [27,50]. These modifications include alterations in concentration of the neutral lipid cholesterol to reduce toxicity, or incorporation of polyethylene glycol (PEG), which reduces aggregations and binding of serum proteins. Targeting peptides should also be considered, for directed uptake into neuroblastoma tumours, as demonstrated in xenografts [51,52], where they can extravasate and concentrate in the tumour, potentially using the enhanced permeation and retention effect [53]. There are numerous further liposome formulations in the clinic or in trials, with a range of biophysical and biochemical properties [25,27,28], so optimised tumour

cell targeting should be achievable. Improved targeting may again facilitate the use of lower systemic doses of retinoic acid in children.

We noted that our empty liposomes appeared to sometimes weakly enhance the effects of ATRA. The liposomes' positive charge could possibly play a role in adsorbing ATRA under some circumstances and future studies could evaluate if neutral or anionic liposomes have similar effects. As an alternative approach, we would also consider co-incorporation of RAMBAs and retinoic acids into cationic liposomes for co-delivery in vivo. This may further reduce off-target toxicities of the retinoids.

In conclusion, hydrophobic RAMBAs derived from imidazole and triazole scaffolds with high specificity for CYP26 enzymes, can be delivered successfully to neuroblastoma cells in liposomes. They enhance the cellular and biochemical actions of RA in SK-N-SH, LAN5, IMR32 and KELLY cells. Not all neuroblastoma tumour cells however will induce CYP26 in response to RA [18] and so, as with most drugs approaches, the benefits of RAMBAs may be restricted to RA-responsive neuroblastoma tumours and resistant tumours where resistance is CYP26 enzyme-based. Use of nanotechnology to deliver RAMBAs could also be considered for applications in other cancers such as basal cell carcinoma [54] , lymphoid malignancies [55] and others, where retinoids are either used clinically or show promise from pre-clinical models [10]. This study has provided a proof of principle and the basis for further investigation of nanotechnology as a delivery pathway for hydrophobic RAMBAs in combination with retinoids, with the goal of increasing the efficacy of retinoid actions in target tissues and improving clinical outcomes.

Acknowledgments

We thank Dale Moulding for his assistance with light microscopy and Image J. This research was supported by Great Ormond Street Children's Charity (grant 2012-NAT-30) and the Medical Research Council UK (EI, PhD Studentship). This research was also supported by

the NIHR Great Ormond Street Hospital Biomedical Research Centre, including support from award 17DD08 for the GOSICH core microscopy facility. The views expressed are those of the authors and not necessarily those of the NHS, the NIHR or the Department of Health.

Declaration of Interest Statement

The authors have no conflict of interest to declare.

References

1. Brodeur GM. Neuroblastoma: biological insights into a clinical enigma. Nat Rev Cancer. 2003 Mar;3(3):203-16.
2. Matthay KK, Reynolds CP, Seeger RC, et al. Long-term results for children with high-risk neuroblastoma treated on a randomized trial of myeloablative therapy followed by 13-cis-retinoic acid: a children's oncology group study. J Clin Oncol. 2009 Mar 1;27(7):1007-13.
3. Sidell N. Retinoic acid-induced growth inhibition and morphologic differentiation of human neuroblastoma cells in vitro. J Natl Cancer Inst. 1982 Apr;68(4):589-96.
4. Janesick A, Wu SC, Blumberg B. Retinoic acid signaling and neuronal differentiation. Cell Mol Life Sci. 2015 Apr;72(8):1559-76.
5. Matthay KK, Villablanca JG, Seeger RC, et al. Treatment of high-risk neuroblastoma with intensive chemotherapy, radiotherapy, autologous bone marrow transplantation, and 13-cis-retinoic acid. Children's Cancer Group. N Engl J Med. 1999 Oct 14;341(16):1165-73.
6. Veal GJ, Errington J, Rowbotham SE, et al. Adaptive dosing approaches to the individualization of 13-cis-retinoic acid (isotretinoin) treatment for children with high-risk neuroblastoma. Clin Cancer Res. 2013 Jan 15;19(2):469-79.

7. Stevison F, Jing J, Tripathy S, et al. Role of Retinoic Acid-Metabolizing Cytochrome P450s, CYP26, in Inflammation and Cancer. Advances in pharmacology (San Diego, Calif). 2015;74:373-412.

8. Nelson CH, Buttrick BR, Isoherranen N. Therapeutic potential of the inhibition of the retinoic acid hydroxylases CYP26A1 and CYP26B1 by xenobiotics. Current topics in medicinal chemistry. 2013;13(12):1402-28.

9. Thatcher JE, Zelter A, Isoherranen N. The relative importance of CYP26A1 in hepatic clearance of all-trans retinoic acid. Biochem Pharmacol. 2010 Sep 15;80(6):903-12.

10. Tang XH, Gudas LJ. Retinoids, retinoic acid receptors, and cancer. Annual review of pathology. 2011;6:345-64.

11. Chapman MS. Vitamin a: history, current uses, and controversies. Seminars in cutaneous medicine and surgery. 2012 Mar;31(1):11-6.

12. Thatcher JE, Isoherranen N. The role of CYP26 enzymes in retinoic acid clearance. Expert opinion on drug metabolism & toxicology. 2009 Aug;5(8):875-86.

13. Veal G, Rowbotham S, Boddy A. Pharmacokinetics and pharmacogenetics of 13-cis-retinoic acid in the treatment of neuroblastoma. Therapie. 2007 Mar-Apr;62(2):91-3.

14. Armstrong JL, Ruiz M, Boddy AV, et al. Increasing the intracellular availability of all-trans retinoic acid in neuroblastoma cells. Br J Cancer. 2005 Feb 28;92(4):696-704.

15. Njar VC. Cytochrome p450 retinoic acid 4-hydroxylase inhibitors: potential agents for cancer therapy. Mini reviews in medicinal chemistry. 2002 Jun;2(3):261-9.

16. Stevison F, Hogarth C, Tripathy S, et al. Inhibition of the all-trans Retinoic Acid (atRA) Hydroxylases CYP26A1 and CYP26B1 Results in Dynamic, Tissue-Specific Changes in Endogenous atRA Signaling. Drug metabolism and disposition: the biological fate of chemicals. 2017 Jul;45(7):846-854.

17. Lopez-Barcons L, Maurer BJ, Kang MH, et al. P450 inhibitor ketoconazole increased the intratumor drug levels and antitumor activity of fenretinide in human neuroblastoma xenograft models. Int J Cancer. 2017 Jul 15;141(2):405-413.

18. Armstrong JL, Taylor GA, Thomas HD, et al. Molecular targeting of retinoic acid metabolism in neuroblastoma: the role of the CYP26 inhibitor R116010 in vitro and in vivo. Br J Cancer. 2007 Jun 04;96(11):1675-83.

19. Gomaa MS, Bridgens CE, Veal GJ, et al. Synthesis and biological evaluation of 3-(1H-imidazol- and triazol-1-yl)-2,2-dimethyl-3-[4-(naphthalen-2-ylamino)phenyl]propyl derivatives as small molecule inhibitors of retinoic acid 4-hydroxylase (CYP26). J Med Chem. 2011 Oct 13;54(19):6803-11.

20. Gomaa MS, Bridgens CE, Illingworth NA, et al. Novel retinoic acid 4-hydroxylase (CYP26) inhibitors based on a 3-(1H-imidazol- and triazol-1-yl)-2,2-dimethyl-3-(4-(phenylamino)phenyl)propyl scaffold. Bioorg Med Chem. 2012 Jul 15;20(14):4201-7.

21. Ocaya P, Gidlof AC, Olofsson PS, et al. CYP26 inhibitor R115866 increases retinoid signaling in intimal smooth muscle cells. Arterioscler Thromb Vasc Biol. 2007 Jul;27(7):1542-8.

22. Miller VA, Rigas JR, Muindi JR, et al. Modulation of all-trans retinoic acid pharmacokinetics by liarozole. Cancer Chemother Pharmacol. 1994;34(6):522-6.

23. Patel JB, Huynh CK, Handratta VD, et al. Novel retinoic acid metabolism blocking agents endowed with multiple biological activities are efficient growth inhibitors of human breast and prostate cancer cells in vitro and a human breast tumor xenograft in nude mice. J Med Chem. 2004 Dec 30;47(27):6716-29.

24. Patel JB, Mehta J, Belosay A, et al. Novel retinoic acid metabolism blocking agents have potent inhibitory activities on human breast cancer cells and tumour growth. Br J Cancer. 2007 Apr 23;96(8):1204-15.

25. Cossu I, Bottoni G, Loi M, et al. Neuroblastoma-targeted nanocarriers improve drug delivery and penetration, delay tumor growth and abrogate metastatic diffusion. Biomaterials. 2015 Nov;68:89-99.

26. Pastorino F, Marimpietri D, Brignole C, et al. Ligand-targeted liposomal therapies of neuroblastoma. Curr Med Chem. 2007;14(29):3070-8.

27. Bulbake U, Doppalapudi S, Kommineni N, et al. Liposomal Formulations in Clinical Use: An Updated Review. Pharmaceutics. Vol. 92017.

28. Parhi P, Mohanty C, Sahoo SK. Nanotechnology-based combinational drug delivery: an emerging approach for cancer therapy. Drug Discov Today. 2012 Sep;17(17-18):1044-52.

29. van der Meel R, Fens MH, Vader P, et al. Extracellular vesicles as drug delivery systems: lessons from the liposome field. Journal of controlled release : official journal of the Controlled Release Society. 2014 Dec 10;195:72-85.

30. Niazi M, Zakeri-Milani P, Najafi Hajivar S, et al. Nano-based strategies to overcome p-glycoprotein-mediated drug resistance. Expert opinion on drug metabolism & toxicology. 2016 Sep;12(9):1021-33.

31. Ganoth A, Merimi KC, Peer D. Overcoming multidrug resistance with nanomedicines. Expert opinion on drug delivery. 2015 Feb;12(2):223-38.

32. Tagalakis AD, Maeshima R, Yu-Wai-Man C, et al. Peptide and nucleic acid-directed self-assembly of cationic nanovehicles through giant unilamellar vesicle modification: Targetable nanocomplexes for in vivo nucleic acid delivery. Acta Biomater. 2017 Mar 15;51:351-362.

33. Huynh CK, Brodie AM, Njar VC. Inhibitory effects of retinoic acid metabolism blocking agents (RAMBAs) on the growth of human prostate cancer cells and LNCaP prostate tumour xenografts in SCID mice. Br J Cancer. 2006 Feb 27;94(4):513-23.

34. Activation of the phosphatidylinositol 3-kinase/Akt signaling pathway by retinoic acid is required for neural differentiation of SH-SY5Y human neuroblastoma cells, (2002).

35. Qiao J, Paul P, Lee S, et al. PI3K/AKT and ERK regulate retinoic acid-induced neuroblastoma cellular differentiation. Biochem Biophys Res Commun. 2012 Aug 03;424(3):421-6.

36. Tagalakis AD, Madaan S, Larsen SD, et al. In vitro and in vivo delivery of a sustained release nanocarrier-based formulation of an MRTF/SRF inhibitor in conjunctival fibrosis. J Nanobiotechnology. 2018 Nov 27;16(1):97.

37. Tagalakis AD, Grosse SM, Meng Q-H, et al. Integrin-targeted nanocomplexes for tumour specific delivery and therapy by systemic administration. Biomaterials. 2011 Mar;32(5):1370-1376.

38. Tagalakis AD, Kenny GD, Bienemann AS, et al. PEGylation improves the receptor-mediated transfection efficiency of peptide-targeted, self-assembling, anionic nanocomplexes. Journal of controlled release : official journal of the Controlled Release Society. 2014 Jan 28;174:177-87.

39. Wada RK, Seeger RC, Reynolds CP, et al. Cell type-specific expression and negative regulation by retinoic acid of the human N-myc promoter in neuroblastoma cells. Oncogene. 1992 Apr;7(4):711-7.

40. Thiele CJ, Reynolds CP, Israel MA. Decreased expression of N-myc precedes retinoic acid-induced morphological differentiation of human neuroblastoma. Nature. 1985 Jan 31-Feb 6;313(6001):404-6.

41. Li Y, Wang J, Gao Y, et al. Relationships between liposome properties, cell membrane binding, intracellular processing, and intracellular bioavailability. The AAPS journal. 2011 Dec;13(4):585-97.

42. Lee KD, Nir S, Papahadjopoulos D. Quantitative analysis of liposome-cell interactions in vitro: rate constants of binding and endocytosis with suspension and adherent J774 cells and human monocytes. Biochemistry. 1993 Jan 26;32(3):889-99.

43. Reynolds CP, Matthay KK, Villablanca JG, et al. Retinoid therapy of high-risk neuroblastoma. Cancer Lett. 2003 Jul 18;197(1-2):185-92.

44. Roenigk HH, Jr. Liver toxicity of retinoid therapy. Pharmacology & therapeutics. 1989;40(1):145-55.

45. Villablanca JG, Khan AA, Avramis VI, et al. Phase I trial of 13-cis-retinoic acid in children with neuroblastoma following bone marrow transplantation. J Clin Oncol. 1995 Apr;13(4):894-901.

46. Muindi J, Frankel SR, Miller WH, Jr., et al. Continuous treatment with all-trans retinoic acid causes a progressive reduction in plasma drug concentrations: implications for relapse and retinoid "resistance" in patients with acute promyelocytic leukemia. Blood. 1992 Jan 15;79(2):299-303.

47. Van Heusden J, Van Ginckel R, Bruwiere H, et al. Inhibition of all-TRANS-retinoic acid metabolism by R116010 induces antitumour activity. Br J Cancer. 2002 Feb 12;86(4):605-11.

48. Veal GJ, Cole M, Errington J, et al. Pharmacokinetics and metabolism of 13-cis-retinoic acid (isotretinoin) in children with high-risk neuroblastoma - a study of the United Kingdom Children's Cancer Study Group. Br J Cancer. 2007 Feb 12;96(3):424-31.

49. Khan AA, Villablanca JG, Reynolds CP, et al. Pharmacokinetic studies of 13-cis-retinoic acid in pediatric patients with neuroblastoma following bone marrow transplantation. Cancer Chemother Pharmacol. 1996;39(1-2):34-41.

50. Allen TM, Cullis PR. Liposomal drug delivery systems: from concept to clinical applications. Adv Drug Deliv Rev. 2013 Jan;65(1):36-48.

51. Tagalakis AD, Lee DH, Bienemann AS, et al. Multifunctional, self-assembling anionic peptide-lipid nanocomplexes for targeted siRNA delivery. Biomaterials. 2014 Sep;35(29):8406-15.

52. Grosse SM, Tagalakis AD, Mustapa MFM, et al. Tumor-specific gene transfer with receptor-mediated nanocomplexes modified by polyethylene glycol shielding and endosomally cleavable lipid and peptide linkers. Faseb J. 2010 Jul;24(7):2301-2313.

53. Danhier F. To exploit the tumor microenvironment: Since the EPR effect fails in the clinic, what is the future of nanomedicine? Journal of controlled release : official journal of the Controlled Release Society. 2016 Dec 28;244(Pt A):108-121.

54. So PL, Fujimoto MA, Epstein EH, Jr. Pharmacologic retinoid signaling and physiologic retinoic acid receptor signaling inhibit basal cell carcinoma tumorigenesis. Mol Cancer Ther. 2008 May;7(5):1275-84.

55. Tsimberidou AM, Giles F, Romaguera J, et al. Activity of interferon-alpha and isotretinoin in patients with advanced, refractory lymphoid malignancies. Cancer. 2004 Feb 1;100(3):574-80.

Figure Legends

Figure 1.

A, RNAseq analysis of LAN5, SK-N-SH (SH), KELLY and IMR32 cells shows the relative amounts of mRNA present for genes *CYP26A1*, *CYP26B1* and *CYP26C1*. mRNA levels after ATRA treatment for 24 h is also shown for LAN5 and SH cells. **B**, chemical structures of compounds C2 and C17, with their respective IC_{50} values against CYP26A1 (Gomaa, M. S., et al. 2011. J Med Chem **54**(19): 6803-6811). **C**, Quantitative PCR was carried out on SK-N-SH cells after treatments with ATRA, RAMBA C2 and C17 and in combinations. Treatments were for 72 h. The relative abundance of *CYP26A1* mRNA is shown, normalised to untreated cells at 1.0. Error bars are standard deviations of triplicate, technical replicates (n=1).

Figure 2.

A, SK-N-SH cells were treated with ATRA alone, or in combination with RAMBA C2 or C17, for 72 h. RAMBAs by themselves had no effect on cell morphology. In combination with ATRA, RAMBAs induce a highly rounded, refractile morphology (insets). Scale bar = 50µm (25µm for insets). **B**, SK-N-SH cells were treated with 0.1µM ATRA and RAMBAs C2 and C17 for 72 h and neurite lengths were measured (n=3). Standard deviations are shown. ANOVA comparisons show where mean neurite lengths are significantly longer compared with ATRA alone (Bonferroni and Dunnet post-hoc corrections *p<0.05; **p<0.01)**.** **C**, SK-N-SH cells were treated for 72 h with ATRA, RAMBA C2 and combinations. Immunoblotting shows relative levels of pAKT and AKT present in cell lysates. **D**, protein bands were quantified and mean pAKT intensities were normalised against AKT and compared using ANOVA (n=3). Controls are untreated cells. SD are shown, **p<0.01 compared to ATRA alone.

Figure 3.

A, SK-N-SH cells were treated for 72 h with 0.1µM ATRA, C17-containing liposomes, or combinations of the two. Controls (con) are untreated and maximal concentrations of RAMBAs are indicated. Neurites were measured and statistical comparison made against the mean of ATRA single treatment. SD are shown, *P<0.05, **p<0.01; n=3. **B**, SK-N-SH cells were treated for 72 h with 0.1µM ATRA, C2-containing liposomes, empty liposomes, and combinations (n=3). SD are shown, *p<0.05, **p<0.01 using ANOVA.

Figure 4.

A, SK-N-SH cells were treated for 72 h with 0.1µM ATRA, 2µM C2 liposomes (C2), 0.5µM C17 liposomes (C17) and combinations thereof. Phase contrast images show that liposomal RAMBAs in combination with ATRA generated highly rounded, neuron-like cells (arrows); 2x enlargements are shown below the main panels. **B**, SK-N-SH cells treated for 72 h with empty liposomes (EL) with or without 0.05µM ATRA, and 0.5µM C17 liposomes plus 0.05µM ATRA. Scale bar = 50µm for rows 2,4 5; 100µM for rows 1 and 3. Maximal, hypothetical concentrations of the RAMBAs are indicated.

Figure 5.

A, SK-N-SH cells were treated for 72 h with ATRA, C17 liposomes (C17 lipo), or combinations. Immunoblotting shows levels of pAKT and AKT; the untreated lane is from the same blot. **B**, a second experiment is shown in which SK-N-SH were treated with ATRA alone, or in combinations with empty liposomes or C2 liposomes (C2 lipo). Immunoblotting of pAKT and AKT are shown. **C,** LAN5 cells were treated for 24 h with 0.1µM ATRA alone and in combinations with empty liposomes and C2-containing liposomes. Immunoblotting shows levels of N-myc and actin. Two independent experiments are shown and maximal, hypothetical concentrations of the RAMBAs are indicated.

Figure 6. SK-N-SH cells were treated with empty liposomes or C2 liposomes for 24 h. The media was then replaced, with and without 0.05μM ATRA, and the cells were cultured for 6 more days. Neurite lengths were measured and means +/- SD are shown (n=3). ANOVA shows significant difference *p<0.05.

Figure 7. A and **B**, KELLY and LAN5 cells were plated in 96-well plates and grown in the presence of a range of concentrations of ATRA or 13-cis-RA. The relative cell survival was measured after 6 days and plotted with means and SD (n=3); zero ATRA is treated as 100% survival. **C** and **D**, Cell proliferation rates were assessed in KELLY and LAN5 cells after treatment for 6 days with zero, 80nM or 160nM ATRA, plus either empty liposomes or C2-containing liposomes at 0.5μM C2 (maximal concentration) (n=3). ANOVA analysis was performed, and SD are shown. *p<0.05; ns, not significant (p>0.05).

Figure 8.

Assessment of the loading and retention of RAMBAs in liposomes. **A**, A UV spectrophotometric scan of 100μM C17 dissolved in ethanol. **B**, table showing independent preparations of liposomes tested for the amount of RAMBA present, expressed as a percentage of the theoretical maximum of 240μM. The percentage of this RAMBA that remained after a 24hr dialysis against distilled water is given, as well as the time delay between liposome synthesis and the dialysis. **C**, Immunoblot of pAKT, AKT and actin from KELLY cells that were treated for 24 h with C2-containing liposomes before (C2) or after (C2-D) dialysis, empty liposomes before (EL) or after (EL-D) dialysis, with or without co-treatment with 0.1μM ATRA (RA).

Supplementary Figure 1. Morphological differentiation of SK-N-SH cells with dialyzed C2 liposomes.

SK-N-SH cells were treated for 6 days with empty liposomes (native and dialyzed), 50µM C2 liposomes (native and dialyzed), 0.05µM ATRA, and combinations thereof. ATRA induces morphological differentiation, whereas addition of C2 liposomes, either native or dialyzed, induces more extreme cell body rounding reflecting mature neurons. Empty liposomes do not induce this more extreme differentiation. Scale bar = 100µm

Supplementary Figure 2. Stimulation of pAKT by both C2 and C17.

Western immunoblots showing pAKT and AKT levels in SKNSH cells after treatments with ATRA and RAMBAs C2 and C17. Cells were treated for 72 hr with 0.1µM ATRA, with and without 0.5µM C2 or 0.5µM C17 (RAMBAs dissolved in ethanol).

Supplementary Figure 3. Dose responses of KELLY and LAN5 cells to ATRA in the presence or absence of liposomes containing C2 RAMBA.

A, an example experiment with KELLY cells plated in triplicate in 96-well plates and treated with a range of ATRA from 2.5µM downwards in 2-fold steps (0.1% final DMSO added to all these wells). To these wells, either C2 liposomes were added to provide 1.1µM C2, or the equivalent quantity of empty liposomes were used to match lipid content. Cells were treated for 7 days before analysis with resazurin. The control c is cells treated with just C2 liposomes (approx. 7µg/ml final lipid); control c1 is cells treated with C2 liposomes plus 0.1% DMSO.

B, A single experiment shown of LAN5 cells treated with a range of ATRA from 5µM downwards in 2-fold steps, in the presence of 0.5µM C2 in liposomes (final concentration of approx. 3.5µg/ml lipids), or empty liposomes. Controls c and c1 are similar to those in **A**. Cells were treated for 5 days before analysis with resazurin.

Supplementary Figure 4. UV scan data of liposomes and RAMBAs

A, example UV scan of 50μM C2 in 100% ethanol. **B**, example UV scan of empty liposomes at 10% w/v in ethanol (effectively 0.1mg/ml lipids). **C,** example scans of c17 liposomes overlaid with empty liposome scans (both at 10% v/v in ethanol). Scans used a 1cm path-length in quartz cuvettes at room temperature.

Table 1. Liposome parameters.

Independent batches of liposomes were made (n, number of batches) and analysed in a Zetasizer Nano ZS for size (diameter in nm), polydispersity index (PDI) and average charge (mV). The standard deviation of each set of batches is given.

Supplementary Table 1. Parameters of liposomes used for RAMBA loading and dialysis studies

Independent batches of liposomes were made containing either C2 or C17. These were analysed in a Zetasizer Nano ZS analyser for parameters of size (mean diameter in nm), polydispersity index (PDI) and average charge (mV).

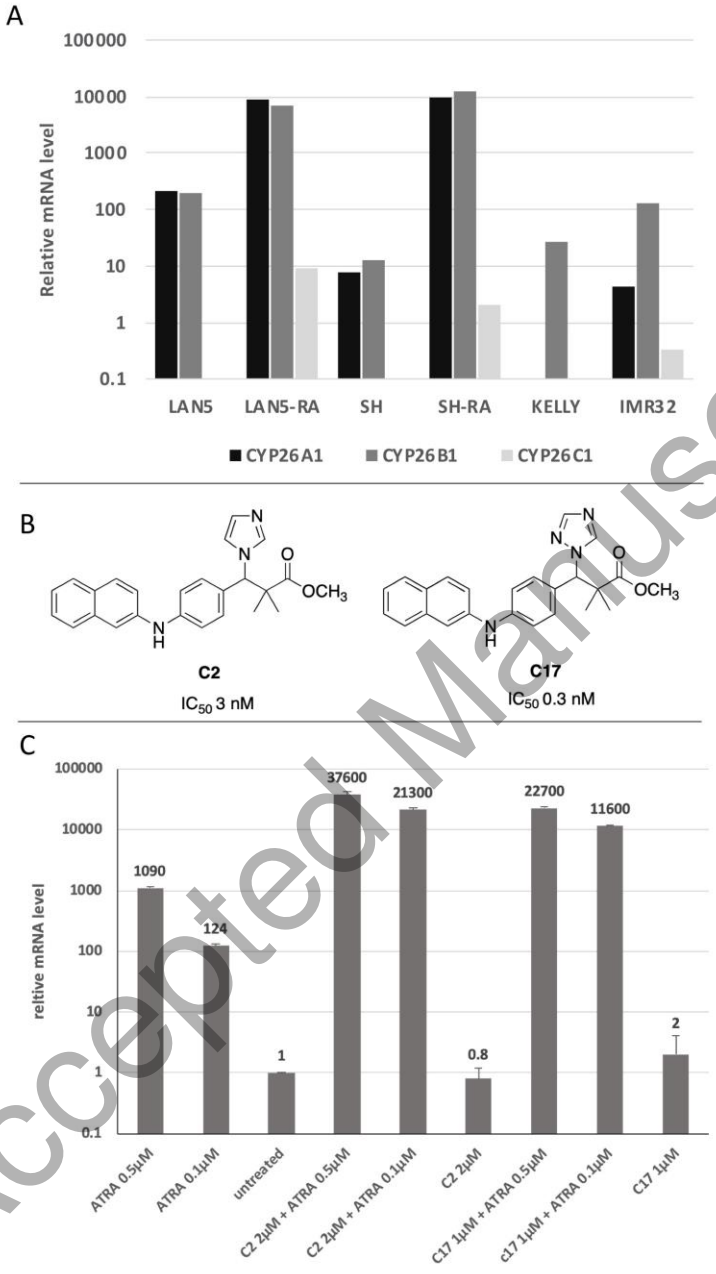

Figure 1

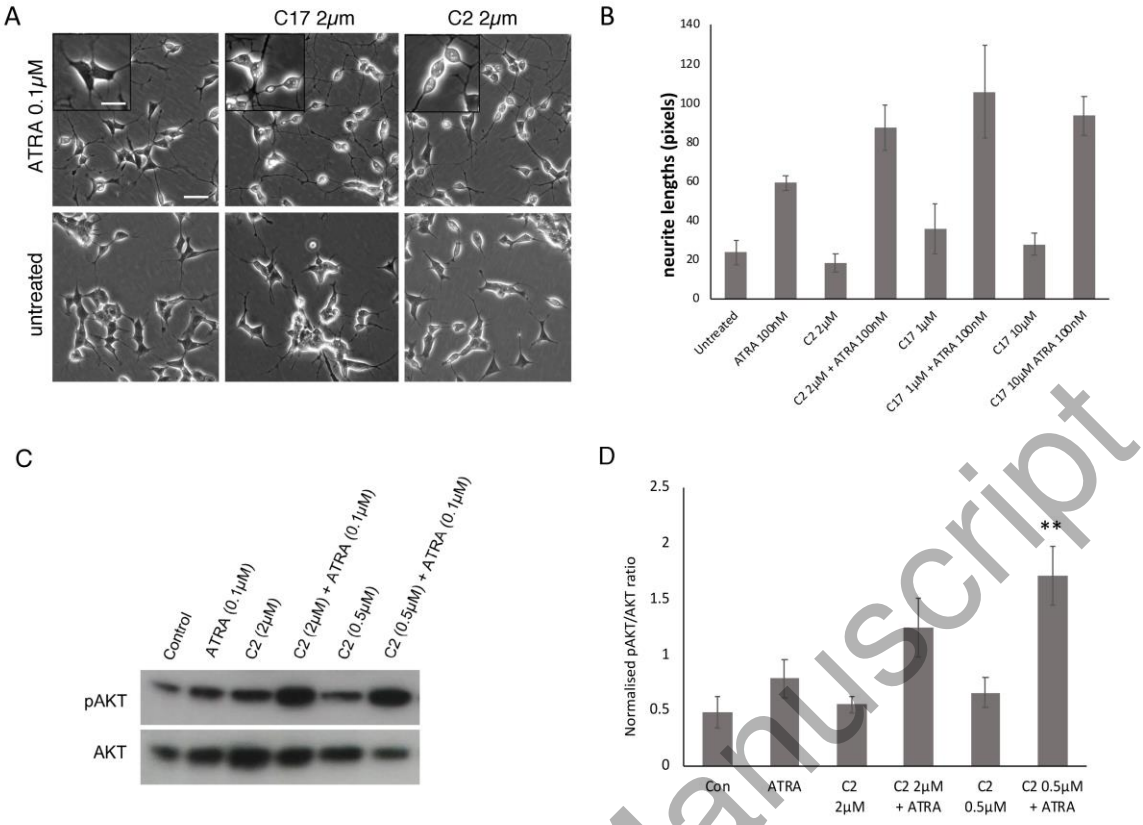

Figure 2

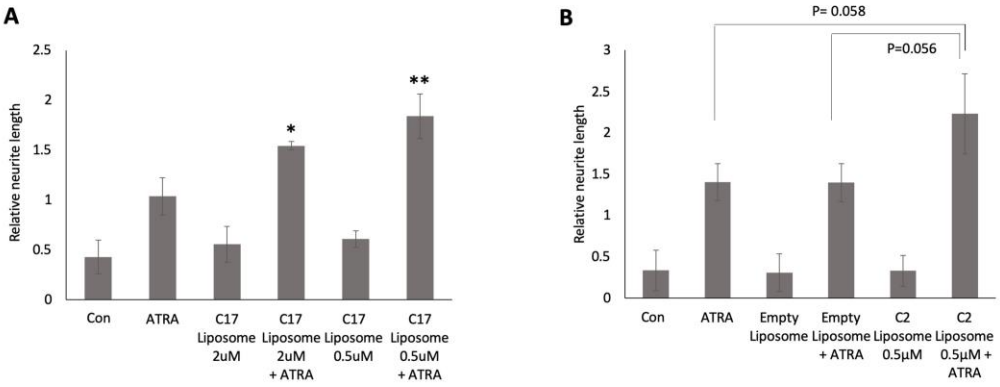

Figure 3

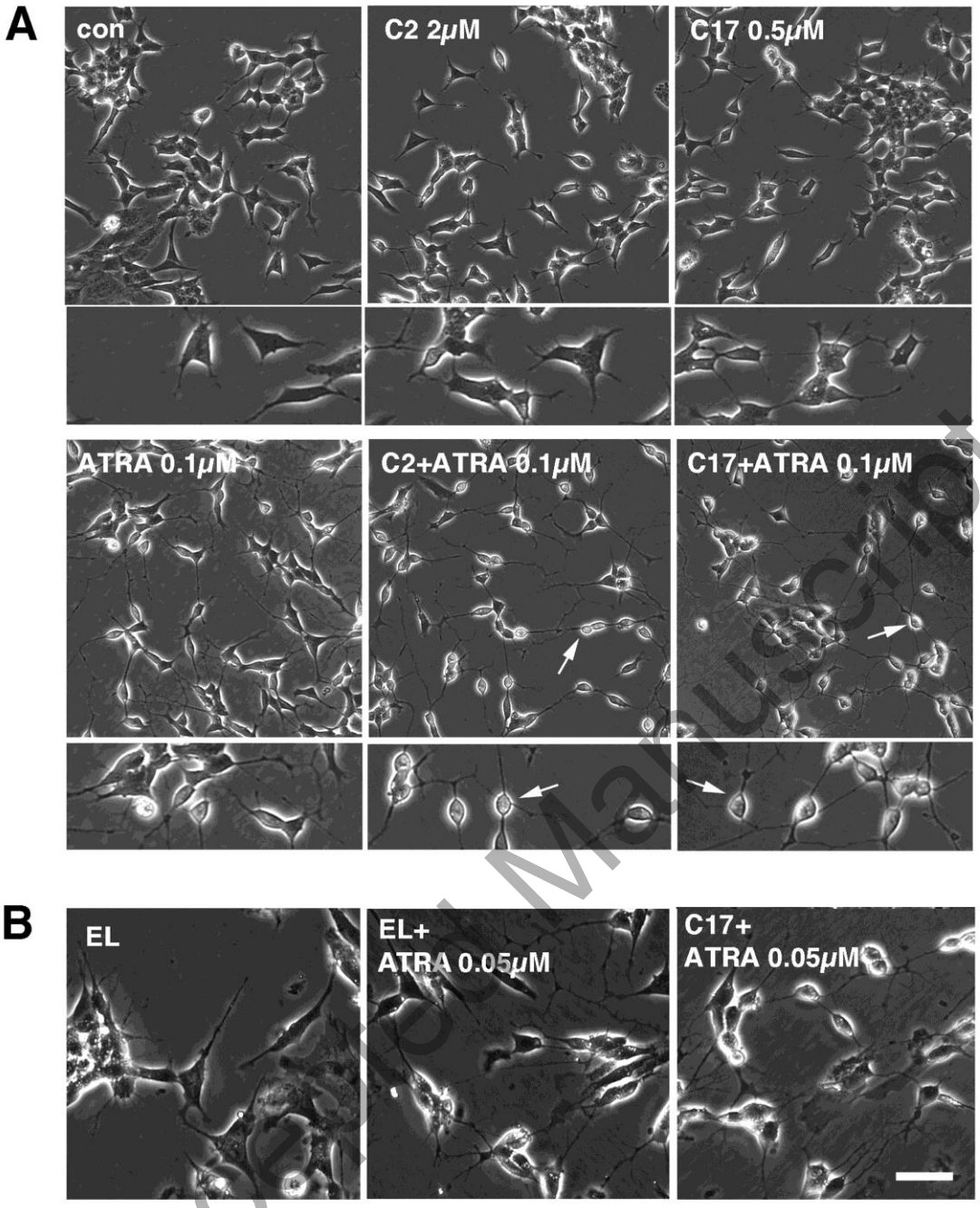

Figure 4

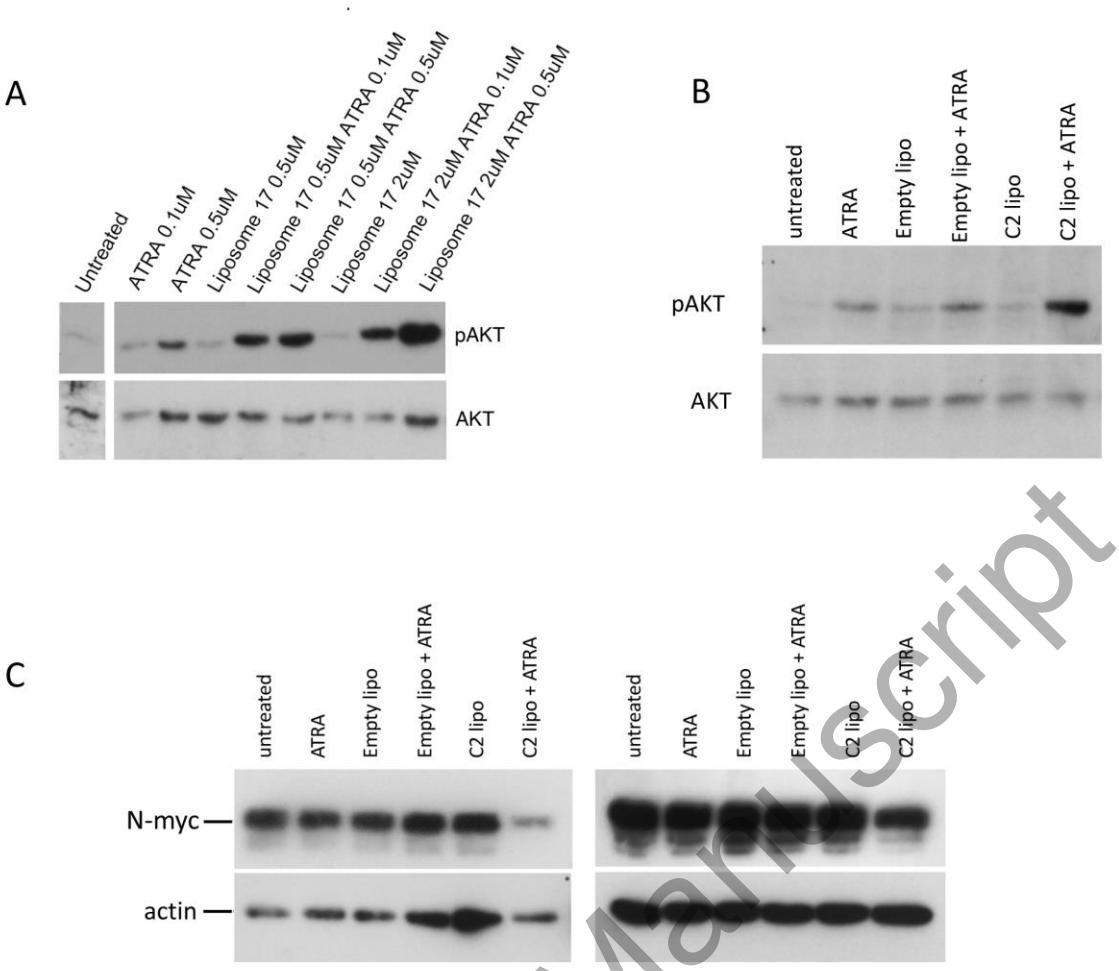

Figure 5

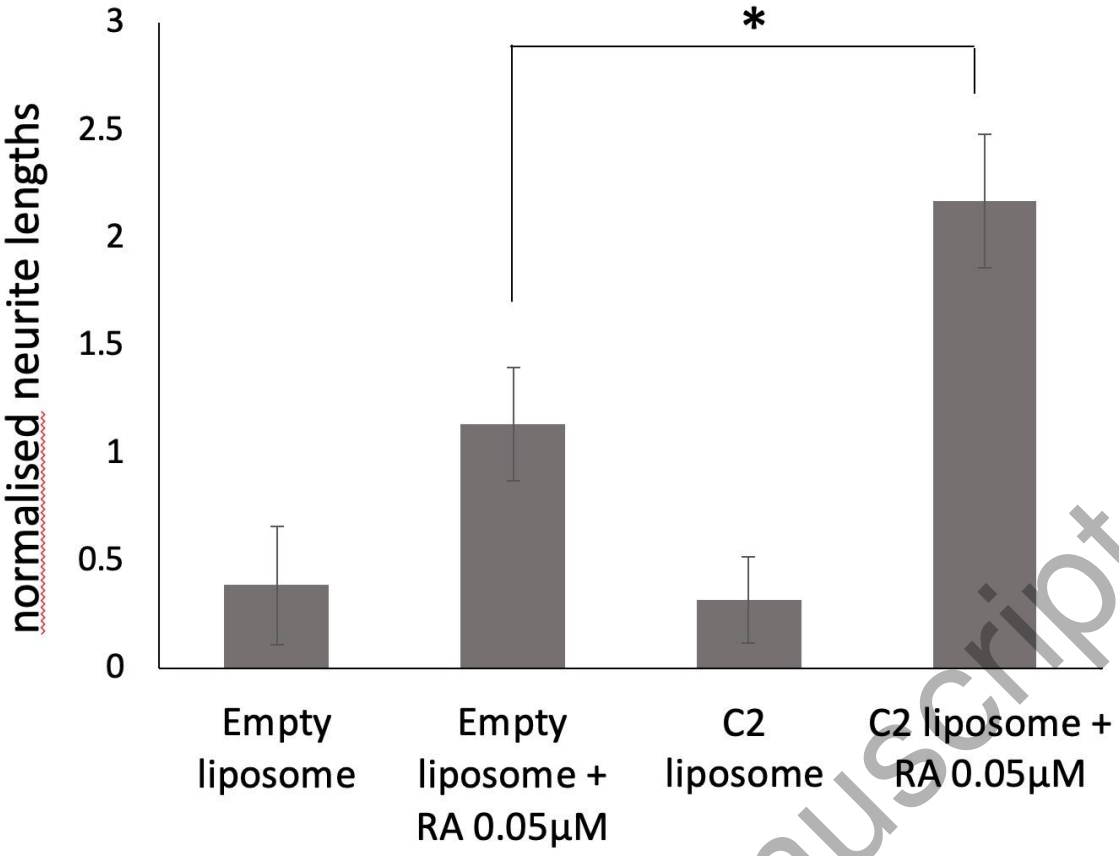

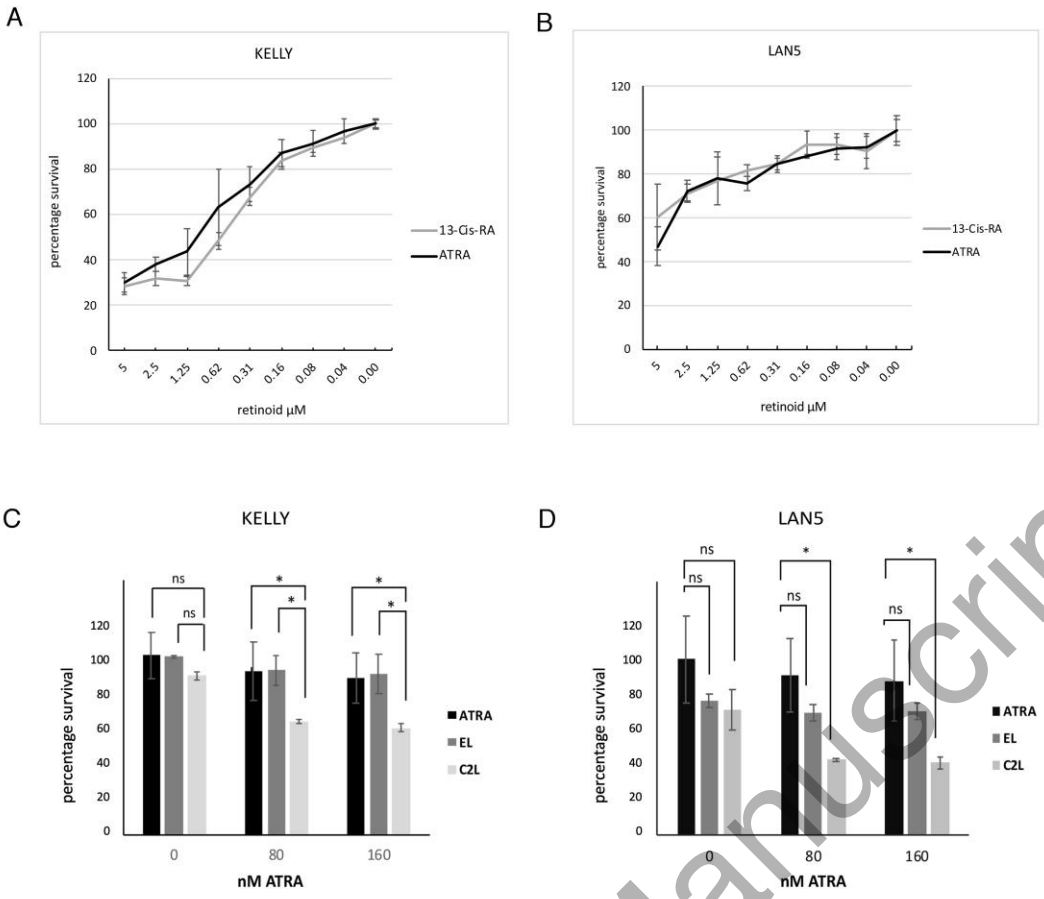

Figure 7

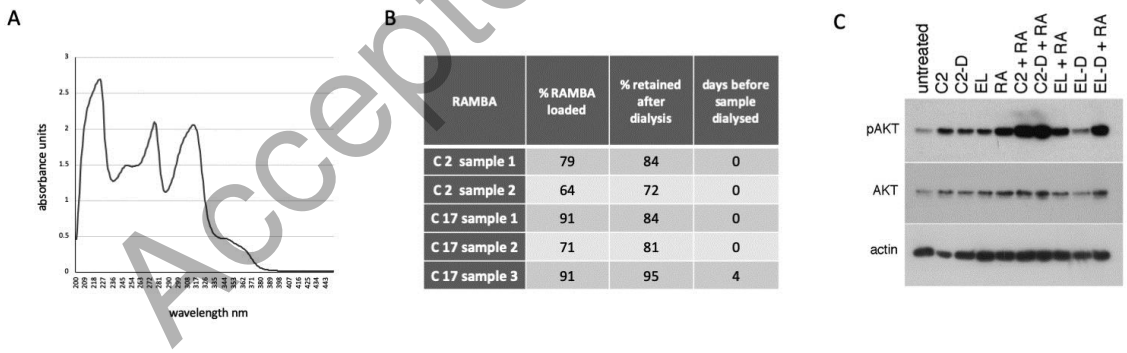

RAMBA	% RAMBA loaded	% retained after dialysis	days before sample dialysed
C 2 sample 1	79	84	0
C 2 sample 2	64	72	0
C 17 sample 1	91	84	0
C 17 sample 2	71	81	0
C 17 sample 3	91	95	4

Figure 8

Table 1. Liposome Parameters

Liposome content	Average Size in nm (range)	SD	Average PDI	SD	Average Charge (mV)	SD
RAMBA C17 (n=3)	90.9 (82-107)	12.3	0.42	0.02	64.0	7.9
RAMBA C2 (n=6)	123.0 (80-164)	30.4	0.42	0.09	62.5	4.6
Empty (n=6)	133 (100-154)	20.5	0.47	0.14	63.0	5.1